Interface Fracture in Layered Materials and Blister Mechanics of Thin Films

Interface Fracture in Layered Materials and Blister Mechanics of Thin Films

By

Simon S. Wang, Christopher M. Harvey and Bo Yuan

Cambridge Scholars Publishing

Interface Fracture in Layered Materials and Blister Mechanics of Thin Films

By Simon S. Wang, Christopher M. Harvey and Bo Yuan

This book first published 2024

Cambridge Scholars Publishing

Lady Stephenson Library, Newcastle upon Tyne, NE6 2PA, UK

British Library Cataloguing in Publication Data
A catalogue record for this book is available from the British Library

ISBN (10): 1-5275-8245-0
ISBN (13): 978-1-5275-8245-3

CONTENTS

ACKNOWLEDGEMENTS

The Authors are extremely grateful to their research students and assistants, particularly: Dr Yingshun Zhang, Dr Chenyu Zhang, Dr Liangliang Guan, Dr Bin Wang, Dr Joseph Wood, Dr Shuo Dai, Dr Matthew Eplett, Dr Tianyu Chen, Dr Vasilis Bagiatis, Harry Hay, Joe Britton, and Oliver Stone, without whom this book would not have been possible. The Authors are also grateful to their colleagues, Prof. Vadim V. Silberschmidt, Prof. Rachel C. Thomson, and Prof. Gary W. Critchlow of Loughborough University; Prof. David Rickerby of Rolls-Royce and Cranfield University; Prof. Huimin Xie of Tsinghua University; and Dr Hongfei Liu at the Institute of Materials Research and Engineering in Singapore. Thanks to Prof. Jiashi Yang for reviewing the book and providing the endorsement. Thanks to John Ingamells of JMI Editorial for the proofreading. In addition, the Authors thank Loughborough University in the UK and Hebei University of Engineering in China for their valuable support to the work reported in this book. Our final thanks go to Dr Jianxin Yin for her help on formatting the manuscript.

CHAPTER 1

INTRODUCTION

1.1 Motivation

Layered materials and thin film coatings are ubiquitous in today's science, engineering, and technology sectors.

Some notable examples are:

- fiber-reinforced composite laminates used in aircraft structures because of their high specific stiffness and strength ratios;
- thermal barrier coatings (TBCs) used in aeroengines and power turbines to increase operating temperatures for higher thermal efficiency;
- submicron-thickness Au films used in the semiconductor industry for fabricating electrodes for electronic devices;
- multilayered Mo/Si mirrors of nanometer thickness used as artificial Bragg structures to reflect light of a specific wavelength in synchrotrons;
- telescope optics;
- extreme ultraviolet optical systems;
- hydrogel films used in tissue and biomedical engineering for novel design of soft microfluidic control systems and soft biomimetic robotics.

The demanding functions and harsh working environments make the inherent weak interfaces in these materials extremely vulnerable to fracture, which directly endangers their integrity and reliability in service and can lead to eventual structural failure. A great deal of research effort has been devoted to studying interface fracture and blister mechanics in these materials over the last few decades; however, academic books on the topic are rare. The authors attempt here to present such a book based on their research work at Loughborough University in the United Kingdom over the last twenty-five years or so. This book aims to gather together some significant advancements on the topic to provide researchers and engineers with more

theoretical tools to study and design such material systems. It contains three major original contributions: (1) doubly orthogonal pure-mode partition theory (DOPPT) for interface mixed-mode fractures in layered materials; (2) blister mechanics of thin films driven by pockets of energy concentration (PECs); and (3) measurements of interface fracture toughness by blister mechanics.

Furthermore, this book can be used as a textbook for advanced courses for postgraduate students and PhD researchers. To facilitate this, each chapter focuses on a relatively independent topic and consists of both theoretical development and experimental applications. Many figures and numerical tables are used to help readers with mechanical understanding and self-practice. Furthermore, the large number of references in the book provides readers with a wide range of background information. A brief introduction to the contents of the book is given below.

1.2 Briefing

Chapters 2 to 5 focus on the DOPPT and experimental and numerical assessments. Chapters 6 to 10 present the blister mechanics of thin films driven by PECs, the studies on the spallation failure of alumina scales, and TBCs in aeroengine turbine blades. In Chapters 11 to 13, the mechanics of telephone cord blisters (TCBs, not to be confused with the similar acronym, TBC) are presented for hard and soft films and verified by using extensive experimental results from the open literature. The mechanics of solitary wave blisters (SWBs) is studied in Chapter 14. Chapters 15 to 19 and the Appendixes focus on the determination of the adhesion toughness of thin films by using blister mechanics and DOPPT. Concluding remarks are given in Chapter 20. Further details about each chapter are given below.

Chapter 2 presents the DOPPT for interface mixed-mode fractures in layered materials. It represents a significant advance in interface fracture mechanics. The DOPPT partitions the total energy release rate (ERR) of 1D interface fractures on brittle homogeneous or bi-material interfaces into its mode-I and mode-II components based on the classical and shear-deformable plate theories and 2D elasticity. Problems that were previously described as “unsolvable” by some are solved, and the points of confusion are explained.

Chapter 3 presents some details of the DOPPT for fiber-reinforced laminated composites with general lay-ups. Several other valuable and popular mixed-mode partition theories are also included. They are assessed against experimental results for the prediction of interface delamination toughness

of fiber-reinforced laminated composites. It is shown that the DOPPT, that is, Wang and Harvey's classical partition theory gives the most accurate predictions; Davidson et al.'s non-singular field partition theory also gives accurate predictions. It is concluded that Wang and Harvey's classical partition theory governs macroscopic interface fracture.

Chapter 4 presents the mechanical theories for studying post-local buckling-driven delamination in layered materials under in-plane compression by utilizing the DOPPT. Independent experimental test data of fiber-reinforced laminates show that the DOPPT based on the classical laminate theory predicts the propagation behavior well.

Chapter 5 presents mixed-mode partition theories for mixed-mode fractures on non-rigid cohesive interfaces by applying DOPPT. Comparisons between theoretical predictions and finite-element method simulations are also presented.

Chapter 6 presents the blister mechanics of thin films based on the hypothesis that delamination of a thin film from a thick substrate is driven by PECs which can be caused by thermal, electrochemical, or other processes. The predictions from the developed model are compared against experimental results and excellent agreement is observed.

Chapter 7 presents studies on the blistering behavior in α-Al_2O_3 scales grown by oxidation on Fe-Cr-Al alloy with different cooling rates. The study shows that non-uniform dynamic creep relaxation can cause pockets of stress concentration around the interface which results in PECs, driving blister formation. The developed mechanical model predicts the blistering behavior in α-Al_2O_3 scales very well.

Chapter 8 presents studies on the spallation behavior of TBCs in aeroengine turbine blades. The topcoat (TC) and the thermally grown oxide (TGO) are considered an effective single material layer. Mechanical models based on the PEC-driven blister mechanics are developed and results of experimental tests are presented. Model predictions are in good agreement with the test results.

Chapter 9 builds on the work described in Chapter 8. Multilayered TBC or functionally graded material systems are considered. A generalized PEC-driven blister mechanics model is developed. Extensive experimental test results are also presented. The predictions from the PEC model are in good agreement with the experiment results.

Chapter 10 presents the details of experimental tests on electron beam physical vapor deposition (EBPVD) TBCs. Two kinds of TBCs are tested:

one with a Pt-modified aluminide bond coat (BC); and another with a Pt-diffused BC. Interface separation is observed to nucleate at the TGO/BC interface, followed by growth and spallation of the blister. It is shown that the failure process occurs under constant residual stress, that is, after cooling to room temperature. Good agreement between the mechanical predictions and the experimental measurements together with microstructural characterization lead to the conclusion that nucleation and spallation of TBC blisters are driven by PECs.

Chapter 11 presents the mechanical theory of TCBs which are frequently observed in film/substrate material systems. They are one of the most interesting instability problems in mechanics. TCBs nucleate and propagate forward with wavy boundaries like worms. The problem has attracted and is still attracting enormous enthusiasm and great effort from many world-leading experts, but it has proved to be extremely challenging. The present study views the problem from a completely new angle: It is discovered that the spontaneous formation and morphology of TCBs in thin films under biaxial compressive residual stresses can be accurately explained and determined by assuming the existence of a PEC instead of the existence of a separation of critical size used in conventional buckling blister mechanics. For the first time, completely analytical formulae, that is, the "Ω formulae," are derived for the two local morphology parameters of TCBs of any shape, that is, width and height, and for the two global morphology parameters of TCBs of sinusoidal shape, that is, the wavelength and transverse amplitude. For the first time, mechanical conditions are also given for the formation of TCBs. Predictions for the four morphology parameters of the developed theory agree very well with extensive experimental results. In addition, by reversing the calculation, the residual stress and the film/substrate interface fracture toughness are also accurately determined from measurements of the TCB morphology parameters. When the parameter Ω, that is, the ratio between the plane strain energy density in the film and the interface fracture toughness, is considerably larger than 3/2, TCB branching can occur and result in hexagonal web blisters (HWBs). The predictions for the size of the HWBs from the Ω formulae have good agreement with experimental test data.

Chapter 12 presents the extension of the TCB mechanical model in Chapter 11 in two respects. Mechanical models are developed for TCBs in multilayered thin films or thin films with functionally graded material properties and, in addition, with large slenderness and waviness ratios. Comparisons between the model predictions and test results are recorded and good agreements are observed.

Chapter 13 presents studies on the TCBs in polymeric hydrogel films. Since hydrogel films undergo dramatic shape and volumetric change when immersed into an appropriate solvent due to swelling or shrinking, experimental studies have observed a variety of instability patterns including TCBs with large slenderness and waviness ratios. The mechanical model in Chapter 12 is utilized to study these TCBs, and accurate predictions are found for the morphology parameters. By introducing the concept of effective interface fracture toughness, the buckling-driven mechanics of TCBs are explained.

Chapter 14 presents studies on the formation and propagation of blisters in MoS_2 thin films on sapphire substrates. Each blister has an axisymmetric shape – with a flat central region and a wave-like upward deflection in the outer region – and propagates like a solitary wave. The study shows that the SWB is a typical PEC-driven blister. A mechanical model is developed, and this explains the SWB behavior.

Chapter 15 presents studies on circular blisters in thin Au films of different thickness on the nanometer scale, deposited by direct current sputtering at room temperature on an Ni-based single crystal (NBSC) superalloy. Transmission electron microscopy (TEM) provides evidence that the blisters nucleate at the Au/NBSC interface. The localized surface adsorption of moisture and its induced interactions during Au-coating result in PECs at the Au/γ-matrix interface in the form of local stress concentration, which causes the formation of circular blisters in thin Au films.

Chapter 16 presents studies on nano circular blisters in multilayered Mo/Si coatings due to bombardment of hydrogen ions. The PEC mechanical model in Chapter 9 is extended and applied to analyze the experimental data. Interface fracture toughness G_{Ic} and G_{IIc} are obtained for different hydrogen ion exposures. The predicted trendlines of blister amplitude vs blister radius are in good agreement with the experimental results.

Chapter 17 presents a study on the ratio of mode-I and mode-II interfacial fracture toughness by using the blister mechanics in Chapters 15 and 16. Its lower and upper bounds are obtained. Extensive experimental results in the open literature are collected and they are in the predicted range.

Chapter 18 presents mechanical models to determine the mode-I and mode-II adhesion toughness, that is, G_{Ic} and G_{IIc}, of monolayer thin films using circular blister tests under either pressure load or point load. The interface fracture of monolayer thin film blisters is mode-I dominant for linear bending with small deflection, while it is mode-II dominant for membrane stretching with large deflection. By taking advantage of the large mode

mixity difference between these two limiting cases, the mode-I and mode-II adhesion toughness are determined in conjunction with a linear failure criterion. Experimental results demonstrate the validity of the method.

Chapter 19 presents studies on adhesion toughness between graphene membranes and substrate. The presence of sliding in multilayered graphene membranes increases the fracture mode mixity G_{II}/G_I, leading to a decrease in adhesion toughness measurements when using the circular blister test under either pressure load or point load. Once the mode-I and mode-II adhesion toughness is known, the adhesion toughness under general service loading conditions can be determined by using mixed-mode partitions based on 2D elasticity and a linear failure criterion.

Chapter 20 gives concluding remarks.

Appendix 1 presents the buckling-driven blister mechanics for straight blisters and pinned circular blisters in thin films with essential formulae.

Appendix 2 presents supplementary information for Chapter 19. It contains the details of the analyses presented in Chapter 19, which are believed to be valuable and particularly helpful to interested readers for applying the mechanical model to their own work. In addition, the details of the DOPPT in Chapter 19 are also presented in the belief that this will also help interested readers to understand the mechanics of the model.

CHAPTER 2

DOUBLY ORTHOGONAL PURE-MODE PARTITION THEORY FOR RIGID INTERFACE FRACTURES

2.1 Introduction

A major concern in the application of layered composite materials is interface fracture during service. This has inspired significant amounts of research into the mechanics of interface fracture under various service conditions. Four well-known fundamental concepts on the topic are the energy release rate (ERR), the stress intensity factor (SIF), the virtual crack closure technique (VCCT), and the J-integral, all of which are well understood. One less well understood fundamental concept is mode mixity, or mixed-mode partition. Mixed-mode partition, however, plays a key role in the mechanics of interface fracture since interface fracture toughness is not a purely intrinsic material property, but instead also depends on mixed-mode partition, that is, the loading conditions at the crack tip. There has been some controversy and confusion around mixed-mode partition over the last few decades. Recently, a powerful doubly orthogonal pure-mode partition theory (DOPPT) (Wang and Harvey, 2012a&b; Harvey and Wang, 2012b; Harvey et al., 2014, 2015b&c; Wood et al., 2016a&b) was developed based on a further understanding of the mechanics of interface fracture. This chapter serves as an introduction to the principles of the DOPPT; the specific details will be presented with practical applications in later chapters.

2.2 Doubly orthogonal pure-mode partition theory (DOPPT)

2.2.1 General theory

Although interface fracture generally occurs as mixed mode with all three opening, shearing, and tearing actions (i.e., mode-I, -II, and -III), 1D interface fracture has received much more attention as it is simpler yet still

captures the essential fracture mechanics. Moreover, analytical solutions can be obtained to provide benchmark results for numerical simulations and calibration formulas for experimental test methods. The expression "1D interface fracture" describes a fracture that propagates in one direction with mode-I and mode-II actions only. Examples of 1D interface fracture are shown in Fig. 2-1, including through-width delamination in double cantilever, straight and curved beams, and blisters in layered plates and shells. As mentioned above, interface fracture toughness depends on the mode mixity at the crack tip. It is often the case that mode-I toughness is the smallest, while the mode-II is the largest. Both are interface intrinsic material properties and are usually determined from experimental tests. A central task in studying 1D interface fracture is to partition the total ERR of a mixed-mode fracture into its individual mode-I and mode-II ERR components. Upon completing the partition, the mixed-mode fracture toughness can be determined by using a fracture propagation criterion and the mode-I and mode-II toughness.

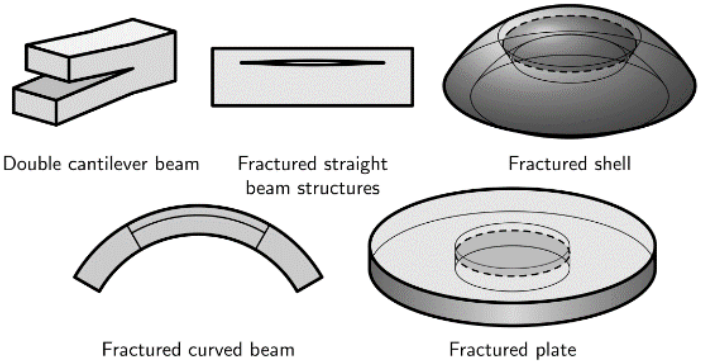

Fig. 2-1: Examples of 1D interface fracture.

Interfaces in many layered materials such as fiber-reinforced laminated composites and multilayered thermal barrier coatings (TBCs) are commonly considered rigid interfaces which produce stress singularities and negligible separations at a crack tip. This chapter focuses on the development of the DOPPT for a mixed-mode fracture on a rigid interface. For a crack on a rigid or brittle interface, the total ERR G at the crack tip represents the difference of strain energy density across the crack tip. For a 1D mixed-mode fracture, ERR can be expressed as

$$G = \{L\}^T[C]\{L\} \tag{2-1}$$

where $\{L\} = \{M_{1B} \quad M_{2B} \quad N_{1B} \quad N_{2B} \quad P_{1B} \quad P_{2B}\}^T$ is the crack tip load vector, comprising the bending moments per unit width M_{1B}, M_{2B}, the axial forces per unit width N_{1B}, N_{2B}, and the shear forces per unit width P_{1B}, P_{2B}, as shown in Fig. 2-2, with the subscripts 1 and 2 denoting the layers above and below the crack and with B denoting the crack tip. The coefficient matrix $[C]$ depends on the material properties, the layups of the layered materials, and the location of the interface fracture. The ERR G in Eq. (2-1) is of quadratic form and non-negative definite in terms of the crack tip load vector.

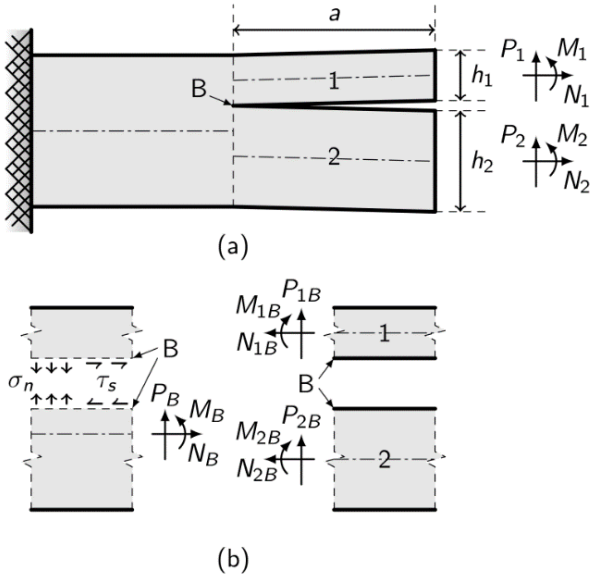

Fig. 2-2: A representative 1D interface fracture model: (a) general description; (b) details local to the crack tip.

By using the VCCT, the individual mode-I and mode-II ERR components, that is, G_I and G_{II} can be written as in the following equations:

$$G_I = \lim_{\Delta a \to 0} \left(\frac{F_n d_n}{2\,\Delta a} \right) \tag{2-2}$$

$$G_{II} = \lim_{\Delta a \to 0} \left(\frac{F_s d_s}{2\,\Delta a} \right) \tag{2-3}$$

where Δa is the crack extension size, F_n and d_n are the crack tip opening force and relative opening displacement, respectively, and F_s and d_s are the

crack tip shearing force and relative shearing displacement, respectively. Clearly, determining F_n, d_n, F_s, and d_s is essential for the calculation of G_I and G_{II}. In the case of the rigid or brittle interface fractures considered here, both F_n and F_s have finite values due to the stress singularity at the crack tip; however, both the relative crack opening and shearing displacements right at the crack tip B are negligible. In the VCCT, that is, Eqs. (2-2) and (2-3), the relative crack tip opening displacement d_n and shearing displacement d_s are measured immediately behind the crack tip B and crack extension self-similarity is assumed. The traditional analytical approach aims to obtain F_n, d_n, F_s, and d_s by solving differential equations. However, the result has limited capabilities and leaves behind some confusion with important problems unsolved.

Recently, the powerful DOPPT was developed. The DOPPT expresses G_I in Eq. (2-2) and G_{II} in Eq. (2-3) as per the following general equations:

$$G_I = c_I \bar{F}_n \bar{d}_n \tag{2-4}$$

with

$$\bar{F}_n = M_{1B} - \frac{M_{2B}}{\beta_1} - \frac{N_{1B}}{\beta_2} - \frac{N_{2B}}{\beta_3} - \frac{P_{1B}}{\beta_4} - \frac{P_{2B}}{\beta_5} \tag{2-5}$$

$$\bar{d}_n = M_{1B} - \frac{M_{2B}}{\beta'_1} - \frac{N_{1B}}{\beta'_2} - \frac{N_{2B}}{\beta'_3} - \frac{P_{1B}}{\beta'_4} - \frac{P_{2B}}{\beta'_5} \tag{2-6}$$

and

$$G_{II} = c_{II} \bar{d}_s \bar{F}_s \tag{2-7}$$

with

$$\bar{d}_s = M_{1B} - \frac{M_{2B}}{\theta_1} - \frac{N_{1B}}{\theta_2} - \frac{N_{2B}}{\theta_3} - \frac{P_{1B}}{\theta_4} - \frac{P_{2B}}{\theta_5} \tag{2-8}$$

$$\bar{F}_s = M_{1B} - \frac{M_{2B}}{\theta'_1} - \frac{N_{1B}}{\theta'_2} - \frac{N_{2B}}{\theta'_3} - \frac{P_{1B}}{\theta'_4} - \frac{P_{2B}}{\theta'_5} \tag{2-9}$$

c_I in Eq. (2-4) and c_{II} in Eq. (2-7) are two constants which are material property-, layup-, and thickness ratio-dependent. When either $\bar{F}_n$ in Eq. (2-5) or $\bar{d}_n$ in Eq. (2-6) equals zero, the mode-I ERR G_I becomes zero, leading to a pure mode-II. $\bar{F}_n$ becomes zero under the following loading conditions:

$$\{L\} = \{1 \quad \beta_1 \quad 0 \quad 0 \quad 0 \quad 0\} \tag{2-10}$$

$$\{L\} = \{1 \quad 0 \quad \beta_2 \quad 0 \quad 0 \quad 0\} \tag{2-11}$$

$$\{L\} = \{1 \quad 0 \quad 0 \quad \beta_3 \quad 0 \quad 0\} \tag{2-12}$$

$$\{L\} = \{1 \quad 0 \quad 0 \quad 0 \quad \beta_4 \quad 0\} \tag{2-13}$$

$$\{L\} = \{1 \quad 0 \quad 0 \quad 0 \quad 0 \quad \beta_5\} \tag{2-14}$$

which are called force-type pure-mode-II modes. Likewise, $\bar{d}_n$ becomes zero under the following loading conditions:

$$\{L\} = \{1 \quad \beta_1' \quad 0 \quad 0 \quad 0 \quad 0\} \tag{2-15}$$

$$\{L\} = \{1 \quad 0 \quad \beta_2' \quad 0 \quad 0 \quad 0\} \tag{2-16}$$

$$\{L\} = \{1 \quad 0 \quad 0 \quad \beta_3' \quad 0 \quad 0\} \tag{2-17}$$

$$\{L\} = \{1 \quad 0 \quad 0 \quad 0 \quad \beta_4' \quad 0\} \tag{2-18}$$

$$\{L\} = \{1 \quad 0 \quad 0 \quad 0 \quad 0 \quad \beta_5'\} \tag{2-19}$$

which are called displacement-type pure-mode-II modes. Similarly, when either $\bar{d}_s$ in Eq. (2-8) or $\bar{F}_s$ in Eq. (2-9) equals zero, the mode-II ERR G_{II} becomes zero, leading to a pure mode-I. $\bar{d}_s$ becomes zero under the following loading conditions:

$$\{L\} = \{1 \quad \theta_1 \quad 0 \quad 0 \quad 0 \quad 0\} \tag{2-20}$$

$$\{L\} = \{1 \quad 0 \quad \theta_2 \quad 0 \quad 0 \quad 0\} \tag{2-21}$$

$$\{L\} = \{1 \quad 0 \quad 0 \quad \theta_3 \quad 0 \quad 0\} \tag{2-22}$$

$$\{L\} = \{1 \quad 0 \quad 0 \quad 0 \quad \theta_4 \quad 0\} \tag{2-23}$$

$$\{L\} = \{1 \quad 0 \quad 0 \quad 0 \quad 0 \quad \theta_5\} \tag{2-24}$$

which are called displacement-type pure-mode-I modes. Likewise, $\bar{F}_s$ becomes zero under the following loading conditions:

$$\{L\} = \{1 \quad \theta_1' \quad 0 \quad 0 \quad 0 \quad 0\} \tag{2-25}$$

$$\{L\} = \{1 \quad 0 \quad \theta_2' \quad 0 \quad 0 \quad 0\} \tag{2-26}$$

$$\{L\} = \{1 \quad 0 \quad 0 \quad \theta_3' \quad 0 \quad 0\} \tag{2-27}$$

$$\{L\} = \{1 \quad 0 \quad 0 \quad 0 \quad \theta_4' \quad 0\} \tag{2-28}$$

$$\{L\} = \{1 \quad 0 \quad 0 \quad 0 \quad 0 \quad \theta_5'\} \tag{2-29}$$

Which are called force-type pure-mode-I modes. All of β_i, β_i', θ_i, and θ_i' ($i = 1, 2, 3, 4, 5$) are material property-, layup-, and thickness ratio-dependent. It is extremely difficult if not impossible to find their analytical expressions using the traditional approach. This is particularly true for finding

analytical expressions for β_i and θ_i' as they are related to the interface stresses with singularity at the crack tip. In the powerful DOPPT, the two most fundamental modes are the displacement-type pure modes in Eqs. (2-15) and (2-20), that is, β_1' pure-mode-II mode and θ_1 pure-mode-I mode. They can be determined analytically, numerically, or experimentally. All the other pure modes in the above equations can then be determined by using the powerful orthogonality principle. That is, for example, by using the following equations to find β_1 and β_2 when θ_1 is known:

$$\{1 \quad \beta_1 \quad 0 \quad 0 \quad 0 \quad 0\}[C]\{1 \quad \theta_1 \quad 0 \quad 0 \quad 0 \quad 0\}^T = 0 \tag{2-30}$$

$$\{1 \quad 0 \quad \beta_2 \quad 0 \quad 0 \quad 0\}[C]\{1 \quad \theta_1 \quad 0 \quad 0 \quad 0 \quad 0\}^T = 0 \tag{2-31}$$

and then using the following equations to find θ_2 and θ_3:

$$\{1 \quad \beta_1 \quad 0 \quad 0 \quad 0 \quad 0\}[C]\{1 \quad 0 \quad \theta_2 \quad 0 \quad 0 \quad 0\}^T = 0 \tag{2-32}$$

$$\{1 \quad \beta_1 \quad 0 \quad 0 \quad 0 \quad 0\}[C]\{1 \quad 0 \quad 0 \quad \theta_3 \quad 0 \quad 0\}^T = 0 \tag{2-33}$$

Similarly, the following equations can be used to find θ_1' and θ_2' when β_1' is known:

$$\{1 \quad \theta_1' \quad 0 \quad 0 \quad 0 \quad 0\}[C]\{1 \quad \beta_1' \quad 0 \quad 0 \quad 0 \quad 0\}^T = 0 \tag{2-34}$$

$$\{1 \quad 0 \quad \theta_2' \quad 0 \quad 0 \quad 0\}[C]\{1 \quad \beta_1' \quad 0 \quad 0 \quad 0 \quad 0\}^T = 0 \tag{2-35}$$

and then using the following equations to find β_2' and β_3':

$$\{1 \quad \theta_1' \quad 0 \quad 0 \quad 0 \quad 0\}[C]\{1 \quad 0 \quad \beta_2' \quad 0 \quad 0 \quad 0\}^T = 0 \tag{2-36}$$

$$\{1 \quad \theta_1' \quad 0 \quad 0 \quad 0 \quad 0\}[C]\{1 \quad 0 \quad 0 \quad \beta_3' \quad 0 \quad 0\}^T = 0 \tag{2-37}$$

(θ_i, β_i) and (θ_i', β_i') $(i = 1, 2, 3, 4, 5)$ are called doubly orthogonal pure modes. Orthogonality exists between any pair in each set. The two sets of orthogonal pure modes are material property-, layup-, and thickness ratio-dependent. More importantly, they depend on the interface properties and the choice of mechanical theory.

2.2.2 DOPPT based on Euler beam or classical plate theory

When Euler beam or classical plate theory is used, Eqs. (2-4) and (2-7) become

$$G_{IE} = c_{IE}\bar{F}_{nE}\bar{d}_{nE} \tag{2-38}$$

$$\bar{F}_{nE} = M_{1B} - \frac{M_{2B}}{\beta_{1-E}} - \frac{N_{1B}}{\beta_{2-E}} - \frac{N_{2B}}{\beta_{3-E}} \tag{2-39}$$

$$\bar{d}_{nE} = M_{1B} - \frac{M_{2B}}{\beta'_{1-E}} - \frac{N_{1B}}{\beta'_{2-\mathrm{E}}} - \frac{N_{2B}}{\beta'_{3-E}} \tag{2-40}$$

$$G_{II\mathrm{E}} = c_{II\mathrm{E}} d_{s\mathrm{E}} F_{s\mathrm{E}} \tag{2-41}$$

$$\bar{d}_{sE} = M_{1B} - \frac{M_{2B}}{\theta_{1-E}} - \frac{N_{1B}}{\theta_{2-E}} - \frac{N_{2B}}{\theta_{3-E}} \tag{2-42}$$

$$\bar{F}_{sE} = M_{1B} - \frac{M_{2B}}{\theta'_{1-E}} - \frac{N_{1B}}{\theta'_{2-E}} - \frac{N_{2B}}{\theta'_{3-E}} \tag{2-43}$$

for both rigid homogeneous and bi-material interfaces, where the subscript E denotes Euler beam or classical plate theory. The two sets of orthogonal pure modes are different from each other, and the through-thickness shearing effects disappear. It was once claimed in the literature that mixed-mode partition was unsolvable based on Euler beam or classical plate theory; however, it is solvable using the powerful DOPPT. In the case of thin-layer delamination, Eqs. (2-38) and (2-41) reduce to

$$G_{IE} = c_{IE}\left(M_{1B} - \frac{N_{1B}}{\beta_{2-E}}\right)\left(M_{1B} - \frac{N_{1B}}{\beta'_{2-E}}\right) \tag{2-44}$$

$$G_{IIE} = c_{IIE}\left(M_{1B} - \frac{N_{1B}}{\theta_{2-E}}\right)\left(M_{1B} - \frac{N_{1B}}{\theta'_{2-E}}\right) \tag{2-45}$$

2.2.3 DOPPT based on Timoshenko beam or first-order shear-deformable plate theory

When a Timoshenko beam or the first-order shear-deformable plate theory is used, Eqs. (2-4) and (2-7) become

$$G_{IT} = c_{IT}\left(M_{1B} - \frac{M_{2B}}{\beta_{1-T}} - \frac{N_{1B}}{\beta_{2-T}} - \frac{N_{2B}}{\beta_{3-T}} - \frac{P_{1B}}{\beta_{4-T}} - \frac{P_{2B}}{\beta_{5-T}}\right)^2 \tag{2-46}$$

$$G_{IIT} = c_{IIT}\left(M_{1B} - \frac{M_{2B}}{\theta_{1-T}} - \frac{N_{1B}}{\theta_{2-T}} - \frac{N_{2B}}{\theta_{3-T}}\right)^2 \tag{2-47}$$

for both rigid homogeneous and bi-material interfaces, where the subscript T denotes a Timoshenko beam or first-order shear-deformable plate theory. The two sets of orthogonal pure modes coincide at the first set of orthogonal pure modes (θ_i, β_i) and the through-thickness shearing effects only produce mode-I ERR. It was thought earlier in the literature that Eqs. (2-38) and (2-41) were equal to Eqs. (2-46) and (2-47), respectively, in the absence of

through-thickness shear forces. The DOPPT clears up this confusion. In the case of thin-layer delamination, Eqs. (2-46) and (2-47) reduce to

$$G_{IT} = c_{IT}\left(M_{1B} - \frac{N_{1B}}{\beta_{2-T}} - \frac{P_{1B}}{\beta_{4-T}}\right)^2 \tag{2-48}$$

$$G_{IIT} = c_{IIT}\left(M_{1B} - \frac{N_{1B}}{\theta_{2-T}}\right)^2 \tag{2-49}$$

2.2.4 DOPPT based on 2D elasticity theory

When 2D elasticity theory is used, Eqs. (2-4) and (2-7) become

$$G_{I2D} = c_{I2D}\left(M_{1B} - \frac{M_{2B}}{\beta_{1-2D}} - \frac{N_{1B}}{\beta_{2-2D}} - \frac{N_{2B}}{\beta_{3-2D}} - \frac{P_{1B}}{\beta_{4-2D}} - \frac{P_{2B}}{\beta_{5-2D}}\right)^2 \tag{2-50}$$

$$G_{II2D} = c_{II2D}\left(M_{1B} - \frac{M_{2B}}{\theta_{1-2D}} - \frac{N_{1B}}{\theta_{2-2D}} - \frac{N_{2B}}{\theta_{3-2D}} - \frac{P_{1B}}{\theta_{4-2D}} - \frac{P_{2B}}{\theta_{5-2D}}\right)^2 \tag{2-51}$$

for rigid homogeneous interfaces where the subscript *2D* denotes 2D elasticity theory. The two sets of orthogonal pure modes coincide with each other and the through-thickness shearing effects produce both mode-I and mode-II ERRs. In the case of thin-layer delamination, Eqs. (2-50) and (2-51) reduce to

$$G_{I2D} = c_{I2D}\left(M_{1B} - \frac{N_{1B}}{\beta_{2-2D}} - \frac{P_{1B}}{\beta_{4-2D}}\right)^2 \tag{2-52}$$

$$G_{II2D} = c_{II2D}\left(M_{1B} - \frac{N_{1B}}{\theta_{2-2D}}\right)^2 \tag{2-53}$$

Note that the through-thickness shearing effects only produce mode-I ERR for thin-layer delamination. For brittle bi-material interfaces, Eqs. (2-4) and (2-7) remain the same, that is,

$$G_{I2D} = c_{I2D}\bar{F}_{n2D}\bar{d}_{n2D} \tag{2-54}$$

$$\bar{F}_{n2D} = M_{1B} - \frac{M_{2B}}{\beta_{1-2D}} - \frac{N_{1B}}{\beta_{2-2D}} - \frac{N_{2B}}{\beta_{3-2D}} - \frac{P_{1B}}{\beta_{4-2D}} - \frac{P_{2B}}{\beta_{5-2D}} \tag{2-55}$$

$$\bar{d}_{n2D} = M_{1B} - \frac{M_{2B}}{\beta'_{1-2D}} - \frac{N_{1B}}{\beta'_{2-2D}} - \frac{N_{2B}}{\beta'_{3-2D}} - \frac{P_{1B}}{\beta'_{4-2D}} - \frac{P_{2B}}{\beta'_{5-2D}} \tag{2-56}$$

$$G_{II2D} = c_{II2D}d_{s2D}F_{s2D} \tag{2-57}$$

$$\bar{d}_{s2D} = M_{1B} - \frac{M_{2B}}{\theta_{1-2D}} - \frac{N_{1B}}{\theta_{2-2D}} - \frac{N_{2B}}{\theta_{3-2D}} - \frac{P_{1B}}{\theta_{4-2D}} - \frac{P_{2B}}{\theta_{5-2D}} \tag{2-58}$$

$$\bar{F}_{s2D} = M_{1B} - \frac{M_{2B}}{\theta'_{1-2D}} - \frac{N_{1B}}{\theta'_{2-2D}} - \frac{N_{2B}}{\theta'_{3-2D}} - \frac{P_{1B}}{\theta'_{4-2D}} - \frac{P_{2B}}{\theta'_{5-2D}} \tag{2-59}$$

The two sets of orthogonal pure modes are not only different from each other but also crack extension size dependent. In the case of thin-layer delamination, Eqs. (2-54) and (2-57) reduce to

$$G_{I2D} = c_{I2D}\left(M_{1B} - \frac{N_{1B}}{\beta_{2-2D}} - \frac{P_{1B}}{\beta_{4-2D}}\right)\left(M_{1B} - \frac{N_{1B}}{\beta'_{2-2D}} - \frac{P_{1B}}{\beta'_{4-2D}}\right) \tag{2-60}$$

$$G_{II2D} = c_{II2D}\left(M_{1B} - \frac{N_{1B}}{\theta_{2-2D}} - \frac{P_{1B}}{\theta_{4-2D}}\right)\left(M_{1B} - \frac{N_{1B}}{\theta'_{2-2D}}\right) \tag{2-61}$$

Finally, it is worth noting that the existence of two sets of orthogonal pure modes in the Euler beam or classical plate partition theory is due to its global nature while the existence of two sets of orthogonal pure modes in 2D elasticity partition theory for brittle bi-material interfaces is due to material mismatch resulting in phase difference in the variation of interface stresses and relative separations. When the extension size Δa is large enough, all three mechanical theories for partition (Euler beam or classical plate theory, Timoshenko or first-order shear-deformable beam theory, and 2D elasticity) unify at the classical partition theory in the absence of the through-thickness shear forces. That is why both the shear-deformable and 2D elasticity partition theories are called local partition theories, while the classical partition theory is called global partition theory. The validity of each theory has been assessed in a series of studies. Details of the orthogonal pure modes (θ_i, β_i) and (θ'_i, β'_i) $(i = 1, 2, 3, 4, 5)$ in each theory can be found in Wang and Harvey (2012a&b), Harvey and Wang (2012b), Harvey et al. (2014, 2015b&c), Wood et al. (2016a&b), and in later chapters.

2.3 Conclusions

While the pure-mode-I and pure-mode-II fracture toughness of an interface are intrinsic material properties, the toughness of a mixed-mode fracture is not, as it also depends on the fracture mode mixity. The total ERR is of quadratic form and non-negative definite in terms of the crack tip loads. The DOPPT provides a powerful analytical methodology to partition the total ERR of 1D mixed-mode fractures into mode-I and mode-II components based on Euler beam or classical plate theory, Timoshenko or first-order shear-deformable beam theory, and 2D elasticity. Problems that were

previously described as “unsolvable” by some are thus solved, and the points of confusion are explained. The DOPPT provides a valuable means for studying interface fracture on the macroscopic, microscopic, and nano scales, and this will be addressed in later chapters.

CHAPTER 3

MIXED-MODE INTERFACE FRACTURES IN LAMINATED COMPOSITES: THEORIES AND EXPERIMENTAL ASSESSMENTS

3.1 Introduction

The partition of mixed-mode fractures is one of the fundamental research topics in the mechanics of interface fractures in layered composite materials. There has been a great deal of confusion concerning it due to the complexities arising from the involvement of many factors such as interface properties, crack extension size, material size, and analytical derivation methodologies, to name only a few. Based on the powerful doubly orthogonal pure-mode partition theory (DOPPT) described in Chapter 2, the authors and their colleagues have carried out a systematic development of partition theories based on classical and shear-deformable beam and plate theories, and 2D elasticity theory, for mixed-mode interface fractures including brittle, cohesive, homogeneous, and bi-material interfaces under general loading conditions (Wang and Harvey, 2012a&b; Harvey and Wang, 2012a&b; Harvey et al., 2015a). Multi-scale interface fractures have been considered, including delamination in macroscopic fiber-reinforced laminated composites, spallation of macroscopic/microscopic thermal barrier coatings (TBCs) in aeroengine turbine blades, spallation of microscopic α-Al_2O_3 films grown by oxidation, telephone cord blisters (TCBs) in microscopic thin films driven by pockets of energy concentration (PEC), and the adhesion toughness of multilayered graphene membranes. Excellent predictions have been observed in comparison with experimental tests. In this chapter, several widely used existing partition theories are introduced and some comparisons are presented for the prediction of interface delamination toughness in macroscopic fiber-reinforced laminated composites.

3.2 Several existing partition theories

Fig. 3-1(a) shows a layered composite double cantilever beam (DCB) with its associated geometry, two crack tip bending moments, and two crack tip axial forces. The partition is based on the bending moments and axial forces acting at the crack tip B, which are shown in Fig. 3-1(b).

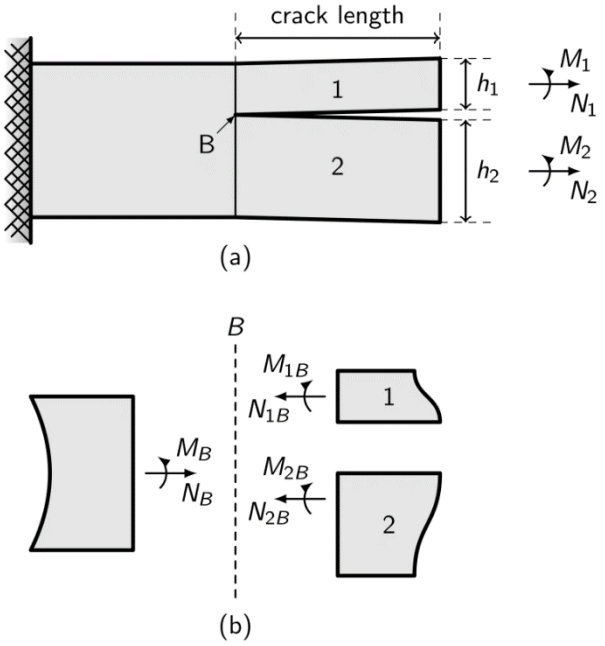

Fig. 3-1: A layered composite DCB: (a) general description; (b) crack tip forces.

3.2.1 The Williams partition theory

Williams was one of the first researchers to attempt to partition a mixed mode (Williams, 1988). His theory was developed for either isotropic materials or unidirectional (UD) composite materials. Williams' partition, denoted by G_{IW} and G_{IIW}, is now reproduced here. For consistency, the notation has been changed where appropriate to match the conventions in this chapter.